Eur. Phys. J. C 50, 519–533 (2007)
DOI 10.1140/epjc/s10052-007-0289-4

THE EUROPEAN PHYSICAL JOURNAL C

Regular Article – Experimental Physics

Probing anomalous Wtb couplings in top pair decays

J.A. Aguilar-Saavedra[1,a], J. Carvalho[2], N. Castro[2], A. Onofre[2,3], F. Veloso[2]

[1] Departamento de Física Teórica y del Cosmos and CAFPE, Universidad de Granada, Campus de Fuentenueva, Edificio Mecenas, 18071 Granada, Spain
[2] LIP – Departamento de Física, Universidade de Coimbra, 3004-516 Coimbra, Portugal
[3] UCP, Rua Dr. Mendes Pinheiro 24, 3080 Figueira da Foz, Portugal

Received: 4 September 2006 / Revised version: 19 December 2006 /
Published online: 5 April 2007 –

Abstract. We investigate several quantities, defined in the decays of top quark pairs, which can be used to explore non-standard Wtb interactions. Two new angular asymmetries are introduced in the leptonic decay of top (anti)quarks. Both are very sensitive to anomalous Wtb couplings, and their measurement allows for a precise determination of the W helicity fractions. We also examine other angular and energy asymmetries, the W helicity fractions and their ratios, as well as spin correlation asymmetries, analysing their dependence on anomalous Wtb couplings and identifing the quantities which are most sensitive to them. It is explicitly shown that spin correlation asymmetries are less sensitive to new interactions in the decay of the top quark; therefore, when combined with the measurement of other observables, they can be used to determine the $t\bar{t}$ spin correlation even in the presence of anomalous Wtb couplings. We finally discuss some asymmetries which can be used to test CP violation in $t\bar{t}$ production and complex phases in the effective Wtb vertex.

1 Introduction

Precision studies have been in the past a powerful tool to explore new physics at scales not kinematically accessible. With the operation of the large hadron collider (LHC), top physics will enter into the era of precise measurements [1]. Due to its large mass, close to the electroweak scale, the top quark is believed to offer a unique window to physics beyond the standard model (SM). New interactions at higher energies may manifest themselves in the form of effective couplings of the SM fermions, especially for the top quark, much heavier than the rest. In this work we concentrate ourselves on the Wtb vertex. Within the SM this coupling is purely left-handed, and its size is given by the Cabibbo–Kobayashi–Maskawa matrix element V_{tb}, which can be measured in single top production [2–5]. In new physics models, departures from the SM expectation $V_{tb} \simeq 1$ are possible [6–8], as well as new radiative contributions to the Wtb vertex [9, 10]. These corrections can be parameterised with the effective operator formalism. The most general Wtb vertex containing terms up to dimension five can be written as

$$\mathcal{L} = -\frac{g}{\sqrt{2}}\bar{b}\gamma^\mu \left(V_{\rm L}P_{\rm L} + V_{\rm R}P_{\rm R}\right) tW_\mu^- - \frac{g}{\sqrt{2}}\bar{b}\frac{{\rm i}\sigma^{\mu\nu}q_\nu}{M_W}\left(g_{\rm L}P_{\rm L} + g_{\rm R}P_{\rm R}\right) tW_\mu^- + {\rm h.c.}\,, \quad (1)$$

with $q = p_t - p_b$ (we follow the conventions of [11] with slight simplifications in the notation). If CP is conserved in the decay, the couplings can be taken to be real.[1] Within the SM, $V_{\rm L} \equiv V_{tb} \simeq 1$ and $V_{\rm R}$, $g_{\rm L}$, $g_{\rm R}$ vanish at the tree level, while nonzero values are generated at one loop level [12]. Additional contributions to $V_{\rm R}$, $g_{\rm L}$, $g_{\rm R}$ are possible in SM extensions, without spoiling the agreement with low-energy measurements. The size of a $V_{\rm R}$ term is constrained by the measured rate of ${\rm Br}(b \to s\gamma) = (3.3 \pm 0.4) \times 10^{-4}$ [13]. A right-handed coupling $|V_{\rm R}| \gtrsim 0.04$ would in principle give a too large contribution to this decay [14–17] which, however, might be (partially) cancelled with other new physics contributions. Hence, the bound $|V_{\rm R}| \leq 0.04$ is model dependent and does not substitute a direct measurement of this coupling. For $g_{\rm L}$ the limits from $b \to s\gamma$ are of the same order, while for $g_{\rm R}$ they are much looser [17].

Top production and decay processes at LHC allow us to probe the Wtb vertex [2, 5, 11, 18, 19]. Top pair production takes place through QCD interactions without involving a Wtb coupling. Additionally, it is likely that the top quark almost exclusively decays in the channel $t \to W^+b$. Therefore, its cross section for production and decay $gg, q\bar{q} \to t\bar{t} \to W^+bW^-\bar{b}$ is insensitive to the size and structure of the Wtb vertex. However, the angular distributions of (anti)top decay products give information about

[a] e-mail: jaas@ugr.es

[1] A general Wtb vertex also contains terms proportional to $(p_t + p_b)^\mu$, q^μ and $\sigma^{\mu\nu}(p_t + p_b)_\nu$. Since b quarks are on shell, the W bosons decay to light particles (whose masses can be neglected) and the top quarks can be approximately assumed on-shell, these extra operators can be rewritten in terms of the ones in (1) using Gordon identities.

its structure, and can then be used to trace non-standard couplings. Angular distributions relating top and antitop decay products probe not only the *Wtb* interactions but also the spin correlations among the two quarks produced, and thus may be influenced by new production mechanisms as well. On the other hand, single top production is sensitive to both the size and structure of the *Wtb* vertex, involved in the production and the decay of the top quark [5, 18, 19].

In this paper we explore the sensitivity of several quantities, like angular and energy asymmetries, helicity fractions and ratios, to new non-standard *Wtb* interactions. Although these observables are theoretically related, the experimental determination is more precise for some of them than for others. In particular, the experimental precision is dominated by systematics already for a luminosity of 10 fb^{-1}, and a good choice of observables can improve significantly the limits on anomalous *Wtb* interactions. Our analysis here is kept at a purely theoretical level, identifying the quantities which are *a priori* more sensitive to anomalous couplings, and estimating the precision in their experimental measurement from a detailed simulation, which has been presented elsewhere [20, 21].

2 W helicity fractions and ratios

The polarisation of the W bosons emitted in the top decay is sensitive to non-standard couplings [22]. The W bosons can be produced with positive (right-handed), negative (left-handed) or zero helicity, with corresponding partial widths $\Gamma_\mathrm{R}, \Gamma_\mathrm{L}, \Gamma_0$, being $\Gamma \equiv \Gamma(t \to W^+ b) = \Gamma_\mathrm{R} + \Gamma_\mathrm{L} + \Gamma_0$. The Γ_R component vanishes in the $m_b = 0$ limit because the b quarks produced in top decays have left-handed chirality, and for vanishing m_b the helicity and the chirality states coincide. The three partial widths can be calculated for a general *Wtb* vertex as parameterised in (1), yielding

$$\begin{aligned}
\Gamma_0 = \frac{g^2|\mathbf{q}|}{32\pi} \Bigg\{ & \frac{m_t^2}{M_W^2} \left[|V_\mathrm{L}|^2 + |V_\mathrm{R}|^2 \right] \\
& \times \left(1 - x_W^2 - 2x_b^2 - x_W^2 x_b^2 + x_b^4\right) - 4x_b \,\mathrm{Re}\, V_\mathrm{L} V_\mathrm{R}^* \\
& + \left[|g_\mathrm{L}|^2 + |g_\mathrm{R}|^2 \right] \left(1 - x_W^2 + x_b^2\right) - 4x_b \,\mathrm{Re}\, g_\mathrm{L} g_\mathrm{R}^* \\
& - 2\frac{m_t}{M_W} \,\mathrm{Re}\left[V_\mathrm{L} g_\mathrm{R}^* + V_\mathrm{R} g_\mathrm{L}^* \right] \left(1 - x_W^2 - x_b^2\right) \\
& + 2\frac{m_t}{M_W} x_b \,\mathrm{Re}\left[V_\mathrm{L} g_\mathrm{L}^* + V_\mathrm{R} g_\mathrm{R}^* \right] \left(1 + x_W^2 - x_b^2\right) \Bigg\} \,, \\
\Gamma_{\mathrm{R,L}} = \frac{g^2|\mathbf{q}|}{32\pi} \Bigg\{ & \left[|V_\mathrm{L}|^2 + |V_\mathrm{R}|^2 \right] \left(1 - x_W^2 + x_b^2\right) - 4x_b \,\mathrm{Re}\, V_\mathrm{L} V_\mathrm{R}^* \\
& + \frac{m_t^2}{M_W^2} \left[|g_\mathrm{L}|^2 + |g_\mathrm{R}|^2 \right] \left(1 - x_W^2 - 2x_b^2 - x_W^2 x_b^2 + x_b^4\right) \\
& - 4x_b \,\mathrm{Re}\, g_\mathrm{L} g_\mathrm{R}^* \\
& - 2\frac{m_t}{M_W} \,\mathrm{Re}\left[V_\mathrm{L} g_\mathrm{R}^* + V_\mathrm{R} g_\mathrm{L}^* \right] \left(1 - x_W^2 - x_b^2\right) \\
& + 2\frac{m_t}{M_W} x_b \,\mathrm{Re}\left[V_\mathrm{L} g_\mathrm{L}^* + V_\mathrm{R} g_\mathrm{R}^* \right] \left(1 + x_W^2 - x_b^2\right) \Bigg\} \\
& \pm \frac{g^2}{64\pi} \frac{m_t^3}{M_W^2} \left\{ -x_W^2 \left[|V_\mathrm{L}|^2 - |V_\mathrm{R}|^2 \right] + \left[|g_\mathrm{L}|^2 - |g_\mathrm{R}|^2 \right] \right. \\
& \times \left(1 - x_b^2\right) + 2x_W \,\mathrm{Re}\left[V_\mathrm{L} g_\mathrm{R}^* - V_\mathrm{R} g_\mathrm{L}^* \right] \\
& \left. + 2x_W x_b \,\mathrm{Re}\left[V_\mathrm{L} g_\mathrm{L}^* - V_\mathrm{R} g_\mathrm{R}^* \right] \right\} \\
& \times \left(1 - 2x_W^2 - 2x_b^2 + x_W^4 - 2x_W^2 x_b^2 + x_b^4\right) \,, \qquad (2)
\end{aligned}$$

being $x_W = M_W/m_t$, $x_b = m_b/m_t$ and

$$\begin{aligned}
|\mathbf{q}| = \frac{1}{2m_t} \Big(& m_t^4 + M_W^4 + m_b^4 - 2m_t^2 M_W^2 \\
& - 2m_t^2 m_b^2 - 2M_W^2 m_b^2 \Big)^{1/2} \qquad (3)
\end{aligned}$$

the modulus of the W boson three-momentum in the top quark rest frame. The total top width is

$$\begin{aligned}
\Gamma = \frac{g^2|\mathbf{q}|}{32\pi} \frac{m_t^2}{M_W^2} \Big\{ & \left[|V_\mathrm{L}|^2 + |V_\mathrm{R}|^2 \right] \\
& \times \left(1 + x_W^2 - 2x_b^2 - 2x_W^4 + x_W^2 x_b^2 + x_b^4\right) \\
& - 12 x_W^2 x_b \,\mathrm{Re}\, V_\mathrm{L} V_\mathrm{R}^* + 2 \left[|g_\mathrm{L}|^2 + |g_\mathrm{R}|^2 \right] \\
& \times \left(1 - \frac{x_W^2}{2} - 2x_b^2 - \frac{x_W^4}{2} - \frac{x_W^2 x_b^2}{2} + x_b^4 \right) \\
& - 12 x_W^2 x_b \,\mathrm{Re}\, g_\mathrm{L} g_\mathrm{R}^* - 6 x_W \,\mathrm{Re}\, \left[V_\mathrm{L} g_\mathrm{R}^* + V_\mathrm{R} g_\mathrm{L}^* \right] \\
& \times \left(1 - x_W^2 - x_b^2\right) \\
& + 6 x_W x_b \,\mathrm{Re}\left[V_\mathrm{L} g_\mathrm{L}^* + V_\mathrm{R} g_\mathrm{R}^* \right] \left(1 + x_W^2 - x_b^2\right) \Big\} \,. \qquad (4)
\end{aligned}$$

The different polarisation states of the W boson are reflected in the angular distribution of its decay products. Let us denote by θ_ℓ^* the angle between the charged lepton three-momentum in the W rest frame and the W momentum in the t rest frame. The normalised differential decay rate for unpolarised top quarks can be written as

$$\begin{aligned}
\frac{1}{\Gamma} \frac{\mathrm{d}\Gamma}{\mathrm{d}\cos\theta_\ell^*} = & \frac{3}{8} (1 + \cos\theta_\ell^*)^2 F_\mathrm{R} + \frac{3}{8} (1 - \cos\theta_\ell^*)^2 F_\mathrm{L} \\
& + \frac{3}{4} \sin^2\theta_\ell^* F_0 \,, \qquad (5)
\end{aligned}$$

with $F_i \equiv \Gamma_i/\Gamma$ the helicity fractions. The three terms correspond to the three helicity states, and the interference terms vanish [23]. At the tree level, $F_0 = 0.703$, $F_\mathrm{L} = 0.297$, $F_\mathrm{R} = 3.6 \times 10^{-4}$, for $m_t = 175\,\mathrm{GeV}$, $M_W = 80.39\,\mathrm{GeV}$, $m_b = 4.8\,\mathrm{GeV}$. The resulting distribution is shown in Fig. 1, calculated from the analytical expressions in (2)–(5) and also with a Monte Carlo simulation. The latter is performed using our own $t\bar{t}$ generator, which uses the full resonant matrix element for $gg, q\bar{q} \to t\bar{t} \to W^+ b W^- \bar{b} \to f_1 \bar{f}_1' b \bar{f}_2 f_2' \bar{b}$, and hence takes into account the top and W widths, as well as their polarisations. Anomalous couplings in the decay may also included in the event generation. We observe that finite width corrections have a negligible influence in the distribution, and hence (2)–(5) can be used to make precise predictions for the distributions.

The good agreement between the analytical calculation (with the top quark and W boson on their mass shell) and the numerical one can be explained substituting $m_t \to m_t(1 + \xi_t\, \Gamma_t/m_t)$, $M_W \to M_W(1 + \xi_W\, \Gamma_W/M_W)$, with ξ_t, ξ_W of order unity, in the expressions of the helicity fractions (here we introduce subscripts to distinguish the

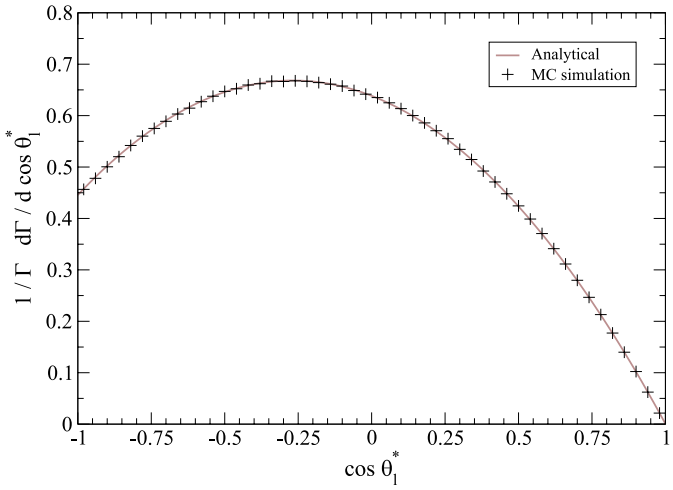

Fig. 1. Differential distribution in (5) within the SM, calculated analytically and with a Monte Carlo simulation

top quark and W boson widths). We obtain

$$
\begin{aligned}
F_0 = 0.703 \Bigg[& 1 + 0.597 \left(\xi_t \frac{\Gamma_t}{m_t}\right) - 0.595 \left(\xi_W \frac{\Gamma_W}{M_W}\right) \\
& - 0.545 \left(\xi_t \frac{\Gamma_t}{m_t}\right)^2 + 0.055 \left(\xi_W \frac{\Gamma_W}{M_W}\right)^2 \\
& + 0.487 \left(\xi_t \frac{\Gamma_t}{m_t}\right) \left(\xi_W \frac{\Gamma_W}{M_W}\right) + \ldots \Bigg] , \\
F_{\rm R} = 3.6 \times 10^{-4} \Bigg[& 1 - 4.48 \left(\xi_t \frac{\Gamma_t}{m_t}\right) + 2.48 \left(\xi_W \frac{\Gamma_W}{M_W}\right) \\
& + 13.22 \left(\xi_t \frac{\Gamma_t}{m_t}\right)^2 + 2.77 \left(\xi_W \frac{\Gamma_W}{M_W}\right)^2 \\
& - 12.98 \left(\xi_t \frac{\Gamma_t}{m_t}\right) \left(\xi_W \frac{\Gamma_W}{M_W}\right) + \ldots \Bigg] , \\
F_{\rm L} = 0.297 \Bigg[& 1 - 1.407 \left(\xi_t \frac{\Gamma_t}{m_t}\right) + 1.405 \left(\xi_W \frac{\Gamma_W}{M_W}\right) \\
& + 1.274 \left(\xi_t \frac{\Gamma_t}{m_t}\right)^2 - 0.134 \left(\xi_W \frac{\Gamma_W}{M_W}\right)^2 \\
& - 1.137 \left(\xi_t \frac{\Gamma_t}{m_t}\right) \left(\xi_W \frac{\Gamma_W}{M_W}\right) + \ldots \Bigg] . \qquad (6)
\end{aligned}
$$

Linear terms have no effect when integrated with symmetric Breit–Wigner distributions, and the quadratic terms are very small.

In the presence of anomalous couplings, the helicity fractions F_i are modified with respect to their SM values quoted above. Their variation is plotted in Fig. 2, considering that only one coupling is different from zero at a time and restricting ourselves to the CP-conserving case of real $V_{\rm R}$, $g_{\rm R}$ and $g_{\rm L}$. We observe that $F_{\rm L}$ and F_0 are much more sensitive to $g_{\rm R}$ than to $g_{\rm L}$ and $V_{\rm R}$. This is due to the interference term $V_{\rm L} g_{\rm R}^*$, which is not suppressed by the bottom quark mass as for the $g_{\rm L}$ and $V_{\rm R}$ couplings. This linear term dominates over the quadratic one and makes the helicity fractions (and related quantities) very sensitive to $g_{\rm R}$. We also remark that the phases of anomalous couplings influence the helicity fractions through the interference terms which depend on the real part of $V_{\rm R}$, $g_{\rm L}$ and $g_{\rm R}$ (we have taken $V_{\rm L}$ real, and normalised to unity). Thus, the effect of complex phases is specially relevant for $g_{\rm R}$, where the interference term dominates. In any case, the maximum and minimum deviations on the helicity fractions are found for real, positive and negative (not necessarily in this order) values of $V_{\rm R}$, $g_{\rm R}$ and $g_{\rm L}$. The possibility of complex couplings is examined with more detail in Sect. 6.

Table 1. 1σ bounds of anomalous couplings obtained from the measurement of helicity fractions F_i and ratios ρ_i

	F_i	ρ_i
$V_{\rm R}$	$[-0.062, 0.13]$	$[-0.029, 0.099]$
$g_{\rm L}$	$[-0.060, 0.028]$	$[-0.046, 0.013]$
$g_{\rm R}$	$[-0.023, 0.021]$	$[-0.025, 0.026]$

The helicity fractions can be experimentally extracted from a fit to the $\cos\theta_\ell^*$ distribution using (5). In order to estimate the limits on anomalous couplings that can be set from their measurement, we assume that the central values obtained correspond to the SM prediction, and take their errors from [20, 21, 24], giving $F_0 \simeq 0.703 \pm 0.016$, $F_{\rm R} \simeq 3.6 \times 10^{-4} \pm 0.0045$, $F_{\rm L} \simeq 0.297 \pm 0.016$. For these values, it is found that F_0 and $F_{\rm L}$ have a similar sensitivity to $g_{\rm R}$, while the dependence of $F_{\rm R}$ on this coupling is smaller. On the other hand, the measurement of $F_{\rm R}$ sets the strongest constraint on $V_{\rm R}$ and $g_{\rm L}$. The resulting bounds are summarised in the first column of Table 1. These and the rest of limits throughout this paper have been obtained with a Monte Carlo method, as described in Appendix B.

The sensitivity achieved for non-standard couplings may be greater if we consider instead the helicity ratios $\rho_{\rm R,L} \equiv \Gamma_{\rm R,L}/\Gamma_0 = F_{\rm R,L}/F_0$, shown in Fig. 3.[2] These ratios can be directly measured with a fit to the $\cos\theta_\ell^*$ distribution as well. From the expected precision in their determination in [20, 21], and assuming that the central values correspond to the SM prediction, we have $\rho_{\rm R} \simeq 0.0005 \pm 0.0026$, $\rho_{\rm L} \simeq 0.423 \pm 0.036$. From these values, the limits given in the second column of Table 1 can be obtained, with an important improvement for $V_{\rm R}$ and $g_{\rm L}$. As it has been remarked in the introduction, the reason for the improvement is that systematic errors, which dominate the precision of the measurements (see [20, 21] for details), are much smaller for helicity ratios than for helicity fractions.

To conclude this section, we would like to stress the importance of keeping the bottom quark mass in the calculations. Within the SM the m_b correction to the helicity fractions is small, of order $x_b^2 = 7.5 \times 10^{-4}$, as it can be seen in (2). However, as it can also be observed, the interference terms involving $g_{\rm L}$ or $V_{\rm R}$ couplings with $V_{\rm L}$ are propor-

[2] We note that, for a better comparison among them and with other observables, the scale of the y axis in each plot is chosen so that the range approximately corresponds to two standard deviations (with the expected LHC precision) around the theoretical SM value.

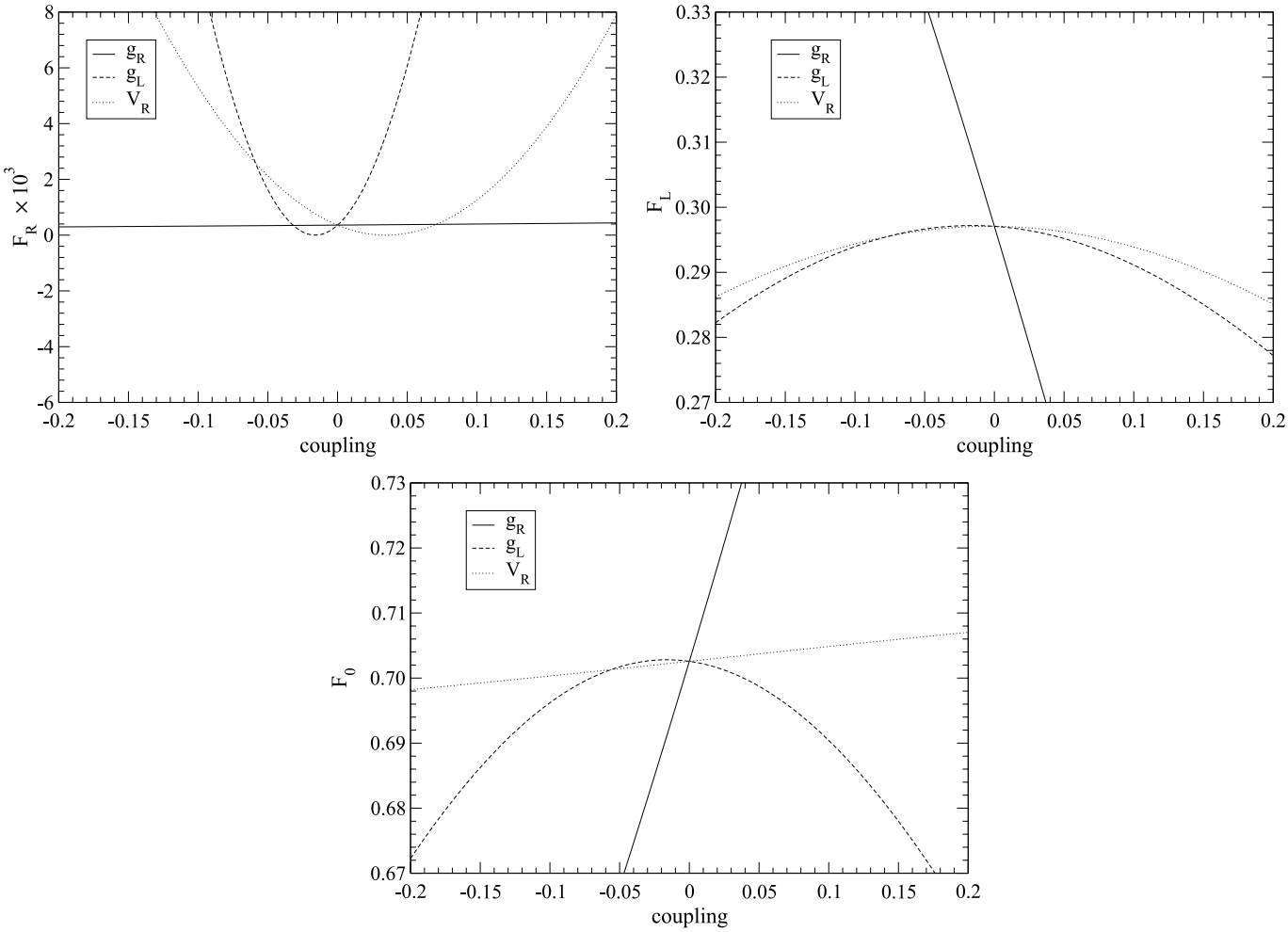

Fig. 2. Dependence of the helicity fractions $F_i = \Gamma_i/\Gamma$ on the anomalous couplings in (1), in the CP-conserving case

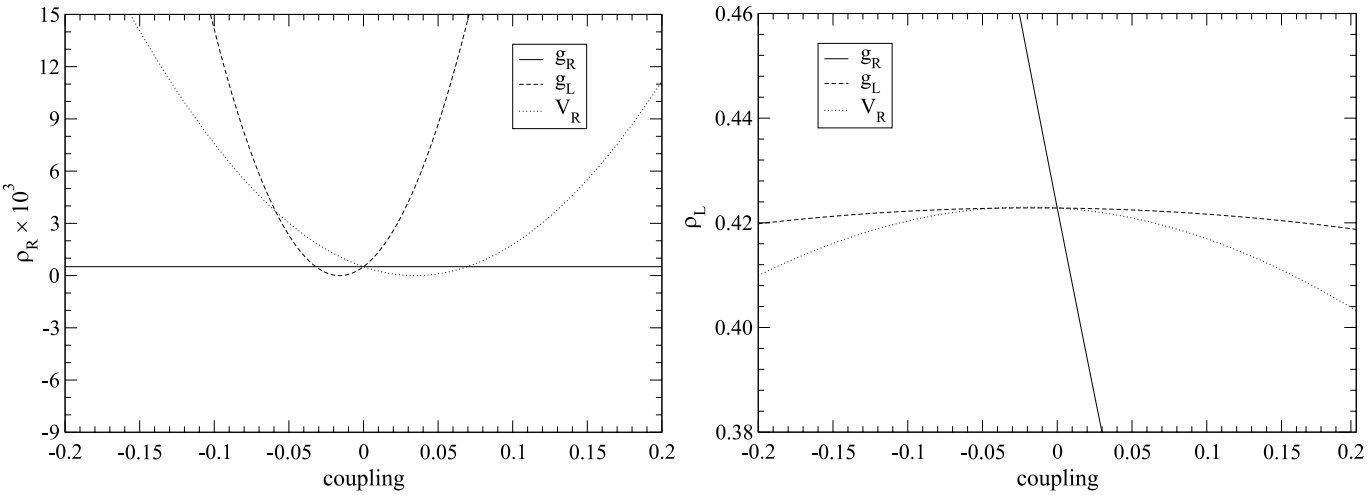

Fig. 3. Dependence of the helicity ratios $\rho_{\rm R,L} = \Gamma_{\rm R,L}/\Gamma_0$ on the anomalous couplings in (1), in the CP-conserving case

tional to $x_b = 0.027$, and are of similar magnitude as the quadratic terms. The effect of including m_b in the computations is illustrated with more detail in Appendix A. Nevertheless, we note here that if m_b is neglected the resulting confidence intervals on $V_{\rm R}$, $g_{\rm L}$ are symmetric. The asymmetry between positive and negative couplings seen in Table 1 reflects the importance of the m_b correction. It should also be noted that the m_b dependence of the limits

leads to a small systematic uncertainty, due to the uncertainty in m_b. This is examined in detail in Appendix A.

3 Angular asymmetries

A simple and efficient method to extract information about the *Wtb* vertex is through angular asymmetries involving the angle θ_ℓ^* between the charged lepton momentum (in the W boson rest frame) and the W^+ boson momentum (in the top quark rest frame). Alternatively, one may consider the angle $\theta_{\ell b}$ between the charged lepton and b quark momenta in the W rest frame. Both approaches are equivalent since these two angles are related by $\theta_\ell^* + \theta_{\ell b} = \pi$. (The determination of $\theta_{\ell b}$, however, is simpler, because both momenta are measured in the same reference frame without any ambiguity in the boosts.) For any fixed z in the interval $[-1, 1]$, one can define an asymmetry

$$A_z = \frac{N(\cos\theta_\ell^* > z) - N(\cos\theta_\ell^* < z)}{N(\cos\theta_\ell^* > z) + N(\cos\theta_\ell^* < z)} \,. \tag{7}$$

The most obvious choice is $z = 0$, giving the forward-backward (FB) asymmetry $A_{\rm FB}$ [11, 25].[3] It is analogous to the FB asymmetries at LEP, which together with the ratios R_b, R_c allow us to extract the couplings of the c and b quarks to the Z boson. The FB asymmetry is related to the W helicity fractions by

$$A_{\rm FB} = \frac{3}{4}[F_{\rm R} - F_{\rm L}] \,. \tag{8}$$

The measurement of this asymmetry alone is not enough to fully reconstruct the $\cos\theta_\ell^*$ distribution. One can then think about other asymmetries for different values of z. The determination of F_i is easier if we construct asymmetries involving only $F_{\rm R}$ and F_0, or $F_{\rm L}$ and F_0. This is achieved choosing $z = \mp(2^{2/3} - 1)$. Defining for convenience $\beta = 2^{1/3} - 1$, we have

$$\begin{aligned} z = -\left(2^{2/3} - 1\right) &\to A_z = A_+ = 3\beta[F_0 + (1+\beta)F_{\rm R}] \,, \\ z = \left(2^{2/3} - 1\right) &\to A_z = A_- = -3\beta[F_0 + (1+\beta)F_{\rm L}] \,. \end{aligned} \tag{9}$$

From both asymmetries and using $F_{\rm R} + F_{\rm L} + F_0 = 1$, we obtain

$$\begin{aligned} F_{\rm R} &= \frac{1}{1-\beta} + \frac{A_- - \beta A_+}{3\beta(1-\beta^2)} \,, \\ F_{\rm L} &= \frac{1}{1-\beta} - \frac{A_+ - \beta A_-}{3\beta(1-\beta^2)} \,, \\ F_0 &= -\frac{1+\beta}{1-\beta} + \frac{A_+ - A_-}{3\beta(1-\beta)} \,. \end{aligned} \tag{10}$$

The three asymmetries $A_{\rm FB}$, A_+, A_- are quite sensitive to anomalous *Wtb* interactions. Their SM values are $A_{\rm FB} = -0.2225$, $A_+ = 0.5482$, $A_- = -0.8397$, and their dependence on the non-standard couplings is shown in Fig. 4. Taking the expected precision in their measurement from [20, 21] and assuming as central values the SM predictions, we obtain $A_{\rm FB} \simeq -0.223 \pm 0.013$, $A_+ \simeq 0.548 \pm 0.010$, $A_- \simeq -0.8397 \pm 0.0033$. Using e.g. the latter two, the helicity fractions can be determined as

$$\begin{aligned} F_{\rm R} &= 0.0017 \pm 0.0071 \,, \\ F_{\rm L} &= 0.2981 \pm 0.0167 \,, \\ F_0 &= 0.7002 \pm 0.0184 \,. \end{aligned} \tag{11}$$

The errors quoted take into account the correlation between the two measurements, which is determined writing the asymmetries in terms of the numbers of events in three bins: $[-1, -(2^{2/3}-1)]$, $[-(2^{2/3}-1), (2^{2/3}-1)]$ and $[(2^{2/3}-1), 1]$. We omit these details for brevity. The values extracted in this way are less precise than if obtained from a direct fit, but the method employed is much simpler too. The eventual limits which would be extracted from asymmetry measurements are collected in Table 2. A_+ exhibits the strongest dependence on $g_{\rm R}$ and, if measured as precisely as it is expected, it would set the best limits on this coupling. On the other hand, A_- is the most sensitive to $V_{\rm R}$ and $g_{\rm L}$ and sets the strongest bounds on them. The limits obtained from asymmetry measurements are competitive with those obtained from a direct fit to the $\cos\theta_\ell^*$ distribution.

Table 2. 1σ bounds on anomalous couplings obtained from the measurement of angular asymmetries

	A_+	A_-	$A_{\rm FB}$
$V_{\rm R}$	$[-0.15, 0.15]$	$[-0.056, 0.11]$	$[-0.12, 0.15]$
$g_{\rm L}$	$[-0.12, 0.082]$	$[-0.057, 0.026]$	$[-0.092, 0.062]$
$g_{\rm R}$	$[-0.019, 0.018]$	$[-0.024, 0.022]$	$[-0.027, 0.025]$

4 Energy distributions

The charged lepton energy in the W rest frame is fixed by the kinematics of the two-body decay $W \to \ell\nu$. Its energy in the top quark rest frame, denoted from now on by E_ℓ, is related to the former by a Lorentz boost, and it is given by

$$E_\ell = \frac{1}{2}(E_W + |\mathbf{q}|\cos\theta_\ell^*) \,, \tag{12}$$

with $|\mathbf{q}|$, given in (3), the W boson momentum in the top rest frame and E_W its energy. Therefore, the angular distribution of the charged lepton in W rest frame determines its energy in the top rest frame. The maximum and minimum energies are $E_{\rm max} = (E_W + |\mathbf{q}|)/2$, $E_{\rm min} = (E_W - |\mathbf{q}|)/2$. The energy distribution is obtained from (5)

[3] Notice the difference in sign with respect to the definitions in [11, 25], where $\theta_{\ell b}$ is used.

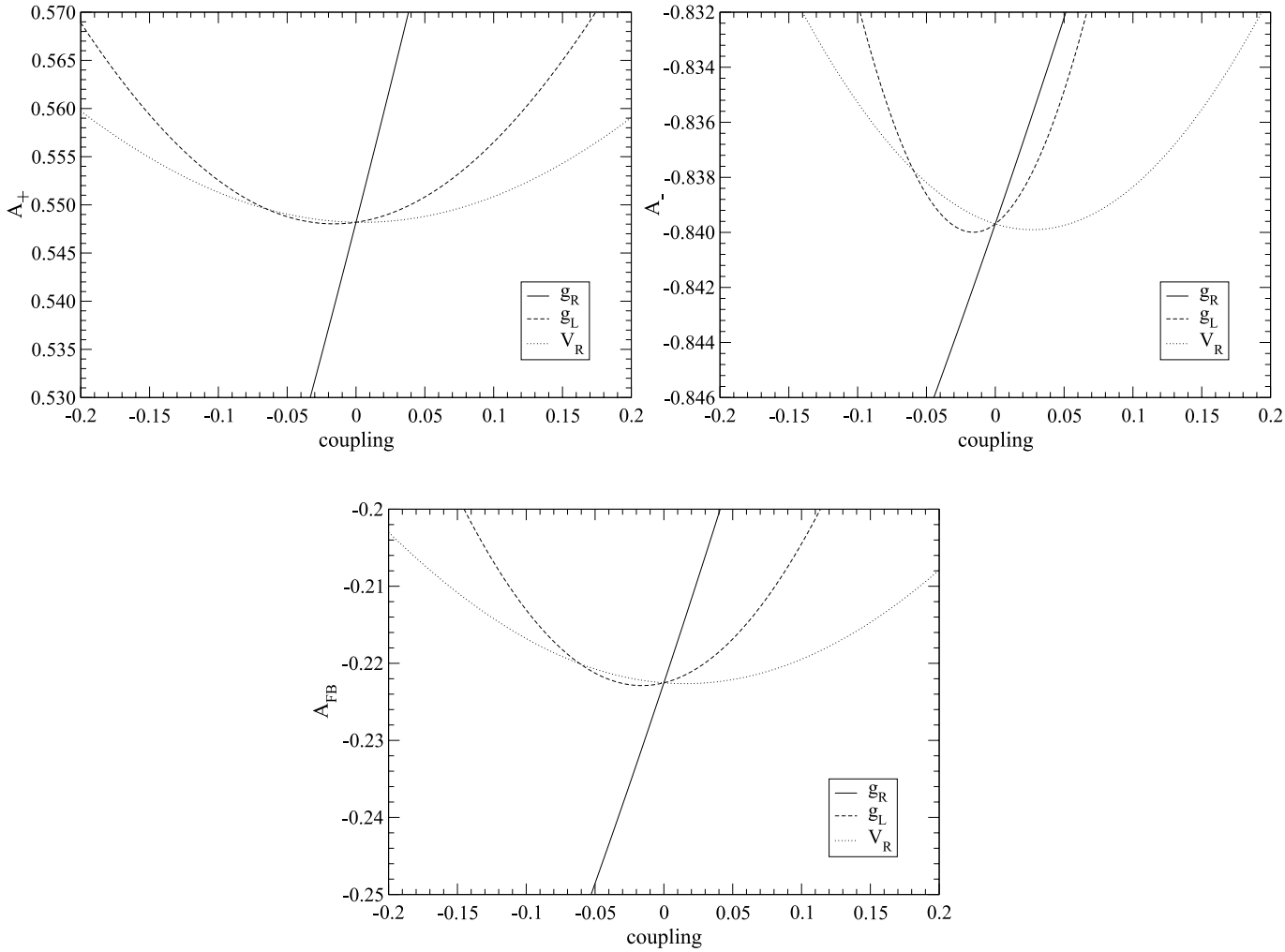

Fig. 4. Dependence of the asymmetries A_+, A_- and $A_{\rm FB}$ on the couplings $g_{\rm L}$, $g_{\rm L}$ and $V_{\rm R}$, for the CP-conserving case

and (12),

$$\frac{1}{\Gamma}\frac{{\rm d}\Gamma}{{\rm d}E_\ell} = \frac{1}{(E_{\rm max}-E_{\rm min})^3} \times \left[3(E_\ell - E_{\rm min})^2 F_{\rm R} + 3(E_{\rm max}-E_\ell)^2 F_{\rm L} + 6(E_{\rm max}-E_\ell)(E_\ell - E_{\rm min}) F_0\right] . \quad (13)$$

The description of the top decay in terms of $\cos\theta_\ell^*$ or E_ℓ seems then equivalent, up to a change of variables. Any asymmetry built using $\cos\theta_\ell^*$, defined around a fixed value z, can be translated into an equivalent asymmetry involving E_ℓ, defined around a fixed energy $E_z = (E_W + |\mathbf{q}|\, z)/2$, namely

$$A_z = \frac{N(E_\ell > E_z) - N(E_\ell < E_z)}{N(E_\ell > E_z) + N(E_\ell < E_z)} . \quad (14)$$

However, in contrast to what was demonstrated in Sect. 2 for the angular distributions, finite width corrections have a non-negligible influence on E_ℓ. This can be seen in Fig. 5, where we plot the energy distribution calculated analytically for t and W on shell and from a Monte Carlo calculation including finite width effects. The values

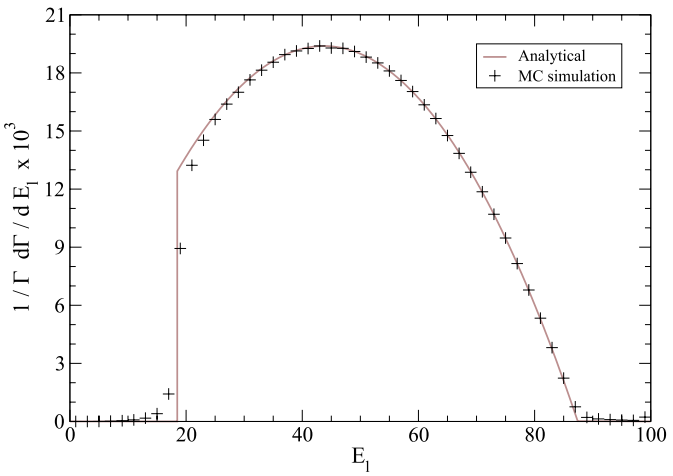

Fig. 5. Differential distribution in (13) within the SM, calculated analytically and with a Monte Carlo simulation

of the asymmetries A_+, A_- and $A_{\rm FB}$, calculated analytically and numerically (the latter for the $\cos\theta_\ell^*$ and E_ℓ distributions) are shown in Table 3. One can notice

Table 3. Values of the asymmetries A_+, A_-, $A_{\rm FB}$ obtained from the analytical expression (first column) and from the Monte Carlo simulation, the latter from the measurement of the distributions of $\cos\theta_\ell^*$ (second column) and E_l (third column)

	Analytical	Angular	Energy
A_+	0.5482	0.5492	0.5529
A_-	−0.8397	−0.8393	−0.8339
$A_{\rm FB}$	−0.2225	−0.2212	−0.2166

the larger influence of finite width corrections for energy asymmetries.

The expected precision in energy asymmetries is worse than for the angular ones (given in the previous section) as it might be expected: $A_{\rm FB} \simeq -0.223 \pm 0.024$, $A_+ \simeq 0.548 \pm 0.013$, $A_- \simeq -0.840 \pm 0.016$. Therefore, in principle their study does not seem to bring any improvement from the experimental side.

5 Spin asymmetries

Additional angular asymmetries can be built involving the top spin. Top quarks are produced unpolarised at the tree level in QCD interactions, and with a very small $O(10^{-2})$ transverse polarisation at one loop. However, the t and $\bar{t}$ spins are strongly correlated, what allows the construction of angular asymmetries at the percent level. The top (anti)quark spins are not directly observable, but influence the angular distribution of their decay products. For the decay $t \to W^+ b \to \ell^+ \nu b, q\bar{q}' b$, the angular distributions of $X = \ell^+, \nu, q, \bar{q}', W^+, b$ (which are called "spin analysers") in the top quark rest frame are given by

$$\frac{1}{\Gamma}\frac{{\rm d}\Gamma}{{\rm d}\cos\theta_X} = \frac{1}{2}(1 + \alpha_X \cos\theta_X) \tag{15}$$

with θ_X the angle between the three-momentum of X (in the t rest frame) and the top spin direction. The constants α_X are called "spin analysing power" of X and can range between -1 and 1. In the SM, $\alpha_{\ell^+} = \alpha_{\bar{q}'} = 1$, $\alpha_\nu = \alpha_q = -0.32$, $\alpha_{W^+} = -\alpha_b = 0.41$ at the tree level [26] (q and q' are the up- and down-type quarks, respectively, resulting from the W decay). For the decay of a top antiquark the distributions are the same, with $\alpha_{\bar{X}} = -\alpha_X$ as long as CP is conserved in the decay. One-loop corrections modify these values to $\alpha_{\ell^+} = 0.998$, $\alpha_{\bar{q}'} = 0.93$, $\alpha_\nu = -0.33$, $\alpha_q = -0.31$, $\alpha_{W^+} = -\alpha_b = 0.39$ [27–29]. We point out that in the presence of non-vanishing $V_{\rm R}$, $g_{\rm L}$ or $g_{\rm R}$ couplings the numerical values of the constants α_X are modified, but the functional form of (15) is maintained. We have explicitly calculated them for a general CP-conserving *Wtb* vertex as written in (1) within the narrow width approximation. They can be written as $\alpha_X = a_X/a_0$, with

$$\begin{aligned}
a_0 = {} & \left[V_{\rm L}^2 + V_{\rm R}^2\right]\left(1 + x_W^2 - 2x_b^2 - 2x_W^4 + x_W^2 x_b^2 + x_b^4\right) \\
& - 12 x_W^2 x_b V_{\rm L} V_{\rm R} \\
& + 2\left[g_{\rm L}^2 + g_{\rm R}^2\right]\left(1 - \frac{x_W^2}{2} - 2x_b^2 - \frac{x_W^4}{2} - \frac{x_W^2 x_b^2}{2} + x_b^4\right) \\
& - 12 x_W^2 x_b g_{\rm L} g_{\rm R} - 6 x_W \left[V_{\rm L} g_{\rm R} + V_{\rm R} g_{\rm L}\right]\left(1 - x_W^2 - x_b^2\right) \\
& + 6 x_W x_b \left[V_{\rm L} g_{\rm L} + V_{\rm R} g_{\rm R}\right]\left(1 + x_W^2 - x_b^2\right) , \\
a_{\ell^+,\bar{q}'} = {} & \left[V_{\rm L}^2 - V_{\rm R}^2\right]\left(1 + x_W^2 - 2x_b^2 - 2x_W^4 + x_W^2 x_b^2 + x_b^4\right) \\
& - 12 x_W^2 x_b V_{\rm L} V_{\rm R} \\
& + 2\left[g_{\rm L}^2 - g_{\rm R}^2\right]\left(1 - \frac{x_W^2}{2} - 2x_b^2 - \frac{x_W^4}{2} - \frac{x_W^2 x_b^2}{2} + x_b^4\right) \\
& - 12 x_W^2 x_b g_{\rm L} g_{\rm R} - 6 x_W \left[V_{\rm L} g_{\rm R} + V_{\rm R} g_{\rm L}\right]\left(1 - x_W^2 - x_b^2\right) \\
& + 6 x_W x_b \left[V_{\rm L} g_{\rm L} - V_{\rm R} g_{\rm R}\right]\left(1 + x_W^2 - x_b^2\right) \\
& + 12 x_W^2 (V_{\rm R}^2 - g_{\rm R}^2) \\
& + \frac{m_t}{|\mathbf{q}|}\log\frac{E_W + |\mathbf{q}|}{E_W - |\mathbf{q}|} \\
& \times \left[-6 x_W^4 V_{\rm R}^2 + 6 x_W^2 g_{\rm R}^2 (1 - x_b^2) + 12 x_W^3 x_b V_{\rm R} g_{\rm R}\right] , \\
a_{\nu,q} = {} & \left[V_{\rm L}^2 - V_{\rm R}^2\right]\left(1 + x_W^2 - 2x_b^2 - 2x_W^4 + x_W^2 x_b^2 + x_b^4\right) \\
& + 12 x_W^2 x_b V_{\rm L} V_{\rm R} \\
& + 2\left[g_{\rm L}^2 - g_{\rm R}^2\right]\left(1 - \frac{x_W^2}{2} - 2x_b^2 - \frac{x_W^4}{2} - \frac{x_W^2 x_b^2}{2} + x_b^4\right) \\
& + 12 x_W^2 x_b g_{\rm L} g_{\rm R} + 6 x_W \left[V_{\rm L} g_{\rm R} + V_{\rm R} g_{\rm L}\right]\left(1 - x_W^2 - x_b^2\right) \\
& + 6 x_W x_b \left[V_{\rm L} g_{\rm L} - V_{\rm R} g_{\rm R}\right]\left(1 + x_W^2 - x_b^2\right) \\
& - 12 x_W^2 (V_{\rm L}^2 - g_{\rm L}^2) \\
& + \frac{m_t}{|\mathbf{q}|}\log\frac{E_W + |\mathbf{q}|}{E_W - |\mathbf{q}|} \\
& \times \left[6 x_W^4 V_{\rm L}^2 - 6 x_W^2 g_{\rm L}^2 (1 - x_b^2) - 12 x_W^3 x_b V_{\rm L} g_{\rm L}\right] , \\
a_b = {} & -2\frac{|\mathbf{q}|}{m_t}\left\{ \left[V_{\rm L}^2 - V_{\rm R}^2\right]\left(1 - 2x_W^2 - x_b^2\right)\right. \\
& + 2\left[g_{\rm L}^2 - g_{\rm R}^2\right]\left(1 - \frac{x_W^2}{2} + x_b^2\right) \\
& \left. + 2 x_W \left[V_{\rm L} g_{\rm R} - V_{\rm R} g_{\rm L}\right] + 6 x_W x_b \left[V_{\rm L} g_{\rm L} - V_{\rm R} g_{\rm R}\right]\right\} ,
\end{aligned} \tag{16}$$

and $a_W = -a_b$. We have checked that our expressions are compatible with the first-order expansions in [30, 31]. Working in the helicity basis and neglecting small spin interference effects, so that the cross section factorises into production times decay factors, the double angular distribution of the decay products X (from t) and $\bar{X}'$ (from $\bar{t}$) can be written as [32]

$$\frac{1}{\sigma}\frac{{\rm d}\sigma}{{\rm d}\cos\theta_X\, {\rm d}\cos\theta_{\bar{X}'}} = \frac{1}{4}(1 + C\alpha_X\alpha_{\bar{X}'}\cos\theta_X\cos\theta_{\bar{X}'}) . \tag{17}$$

The angles $\theta_X, \theta_{\bar{X}'}$ are measured using as spin axis the parent top (anti)quark momentum in the $t\bar{t}$ CM system. The factor

$$C \equiv \frac{\sigma(t_{\rm R}\bar{t}_{\rm R}) + \sigma(t_{\rm L}\bar{t}_{\rm L}) - \sigma(t_{\rm R}\bar{t}_{\rm L}) - \sigma(t_{\rm L}\bar{t}_{\rm R})}{\sigma(t_{\rm R}\bar{t}_{\rm R}) + \sigma(t_{\rm L}\bar{t}_{\rm L}) + \sigma(t_{\rm R}\bar{t}_{\rm L}) + \sigma(t_{\rm L}\bar{t}_{\rm R})} \tag{18}$$

is the relative number of like helicity minus opposite helicity $t\bar{t}$ pairs, and measures the spin correlation between the

top quark and antiquark.[4] We note that due to P invariance of the QCD interactions, $\sigma(t_\mathrm{R}\bar{t}_\mathrm{L}) = \sigma(t_\mathrm{L}\bar{t}_\mathrm{R})$, and by CP conservation $\sigma(t_\mathrm{R}\bar{t}_\mathrm{R}) = \sigma(t_\mathrm{L}\bar{t}_\mathrm{L})$. This is the reason why terms linear in $\cos\theta_X$, $\cos\theta_{\bar{X}'}$ are absent in (17). In other words, terms linear in the cosines are present only if the top quarks are produced with a net polarisation in the helicity basis, what does not happen in pure QCD production. The actual value of C depends to some extent on the parton distribution functions (PDFs) used and the Q^2 scale at which they are evaluated. Using the CTEQ5L PDFs [34] and $Q^2 = \hat{s}$ the partonic CM energy, we find $C = 0.310$. At the one loop level, $C = 0.326 \pm 0.012$ [29].

Using the spin analysers X, $\bar{X}'$ for the respective decays of t, $\bar{t}$, one can define the asymmetries

$$A_{X\bar{X}'} \equiv \frac{N(\cos\theta_X \cos\theta_{\bar{X}'} > 0) - N(\cos\theta_X \cos\theta_{\bar{X}'} < 0)}{N(\cos\theta_X \cos\theta_{\bar{X}'} > 0) + N(\cos\theta_X \cos\theta_{\bar{X}'} < 0)}\,, \tag{19}$$

whose theoretical value derived from (17) is

$$A_{X\bar{X}'} = \frac{1}{4} C \alpha_X \alpha_{\bar{X}'}\,. \tag{20}$$

If CP is conserved in the decay, for charge conjugate decay channels we have $\alpha_{X'}\alpha_{\bar{X}} = \alpha_X \alpha_{\bar{X}'}$, so the asymmetries $A_{X'\bar{X}} = A_{X\bar{X}'}$ are equivalent. Therefore, we can sum both channels and drop the superscripts indicating the charge, denoting the asymmetries by $A_{\ell\ell'}$, $A_{\nu\ell'}$, etc. (CP-violating effects will be discussed in the next section). In semileptonic top decays we can select as spin analyser the charged lepton, which has the largest spin analysing power, or the neutrino, as proposed in [35]. In hadronic decays the jets corresponding to up- and down-type quarks are very difficult to distinguish, and one possibility is to use the least energetic jet in the top rest frame, which corresponds to the down-type quark 61% of the time, and has a spin analysing power $\alpha_j = 0.49$ at the tree level. An equivalent possibility is to choose the d jet by its angular distribution in the W^- rest frame [33]. In both hadronic and leptonic decays the b ($\bar{b}$) quarks can be used as well.

In the lepton + jets decay mode of the $t\bar{t}$ pair, $t\bar{t} \to \ell\nu bjj\bar{b}$ we choose the two asymmetries $A_{\ell j}$, $A_{\nu j}$, for which we obtain the SM tree-level values $A_{\ell j} = -0.0376$, $A_{\nu j} = 0.0120$. With the precision expected for their measurement at LHC [21], the measurements $A_{\ell j} \simeq -0.0376 \pm 0.0058$, $A_{\nu j} \simeq 0.0120 \pm 0.0056$ are feasible. The dependence of these asymmetries on anomalous *Wtb* couplings is depicted in Fig. 6 (we remind the reader that the y axis scales are chosen so that the range approximately corresponds to two standard deviations around the theoretical SM value). These plots are obtained using (16) and (20). We have checked, using high-statistics Monte Carlo simulations, that finite width effects are rather small, so that (16) and (20) can be used to make accurate predictions for spin correlation asymmetries. In the dilepton channel $t\bar{t} \to \ell\nu b\ell'\nu\bar{b}$ we select the asymmetries $A_{\ell\ell'}$, $A_{\nu\ell'}$, whose SM values are $A_{\ell\ell'} = -0.0775$, $A_{\nu\ell'} = 0.0247$. The uncertainty in their measurement can be estimated from [21, 24], yielding $A_{\ell\ell'} \simeq -0.0775 \pm 0.0060$, $A_{\nu\ell'} \simeq 0.0247 \pm 0.0087$. Their variation when anomalous couplings are present is shown in Fig. 6. We also plot (in this case with arbitrary y axis scales) the asymmetries A_{lb}, A_{bb}, which can be measured either in the semileptonic or dilepton channel. Their SM values are $A_{lb} = 0.0314$, $A_{bb} = -0.0128$, but the experimental sensitivity has been not estimated as yet. We expect that it may be of the order of 10% for A_{lb}, and worse for A_{bb}.

The comparison of these plots with the ones in previous sections makes apparent that, given the experimental accuracies achievable in each case, spin correlation asymmetries are much less sensitive to non-standard *Wtb* couplings. This implies that, if no deviations are found in the measurement of the helicity ratios $\rho_\mathrm{R,L}$ and angular asymmetries $A_\pm$, spin-dependent asymmetries can be used to test $t\bar{t}$ spin correlations in the production, without contamination from possible new interactions in the decay. In particular, this is the case of $A_{\ell\ell'}$ and $A_{\ell j}$, whose relative accuracy is better, 7.7% and 15%, respectively. The determination of the correlation factor C in (18) from these asymmetries would eventually give

$$\begin{aligned} A_{\ell\ell'} \to C = 0.310 &\pm 0.024\,(\mathrm{exp})\,{}^{+0.}_{-0.0043}\,(\delta V_\mathrm{R}) \\ &{}^{+1\times10^{-5}}_{-3\times10^{-6}}(\delta g_\mathrm{L})\,{}^{+7\times10^{-6}}_{-0.0004}\,(\delta g_\mathrm{R})\,, \\ A_{\ell j} \to C = 0.310 &\pm 0.045\,(\mathrm{exp})\,{}^{+0.}_{-0.0068}\,(\delta V_\mathrm{R}) \\ &{}^{+0.0001}_{-0.0008}(\delta g_\mathrm{L})\,{}^{+0.0004}_{-0.0009}\,(\delta g_\mathrm{R})\,. \end{aligned} \tag{21}$$

The first error quoted corresponds to the experimental (systematic and statistic) uncertainty. The other ones are theoretical uncertainties obtained varying the anomalous couplings (one at a time). The confidence level (CL) corresponding to the intervals quoted is 68.3%. The numerical comparison of the different terms in (21) also shows that $A_{\ell j}$ and $A_{\ell\ell'}$ are much less sensitive to non-standard top couplings than A_+, A_- and $\rho_\mathrm{R,L}$. It must also be noted that, since all asymmetries depend on the production mechanism through the common factor C, their ratios do not (to leading order), and hence they are clean probes for anomalous couplings. The precision in the measurement of asymmetry ratios is still to be determined, but at any rate it is expected to be worse than for spin-independent observables discussed in the previous sections.

It is also interesting to study the relative distribution of one spin analyser from the t quark and other from the $\bar{t}$. Let $\varphi_{X\bar{X}'}$ be the angle between the three-momentum of X (in the t rest frame) and of $\bar{X}'$ (in the $\bar{t}$ rest frame). The angular distribution can be written as [29]

$$\frac{1}{\sigma}\frac{\mathrm{d}\sigma}{\mathrm{d}\cos\varphi_{X\bar{X}'}} = \frac{1}{2}(1 + D\alpha_X\alpha_{\bar{X}'}\cos\varphi_{X\bar{X}'})\,, \tag{22}$$

with D a constant defined by this equality. In our simulations we obtain the tree-level value $D = -0.217$, while at

[4] Other conventions in the literature (e.g. [29, 33]) denote by $-C$ what in our case is the product $C\,\alpha_X\alpha_{\bar{X}'}$. We prefer to keep the notation in [1, 32] and separate the contributions from the production (C) and the decay (α_X, $\alpha_{\bar{X}'}$) since the former is sensitive to new physics in the $t\bar{t}$ production process while the latter are sensitive to non-standard *Wtb* interactions. This decomposition is not possible if non-factorisable radiative corrections to the production and decay process are included. Anyway, these corrections are expected to be small.

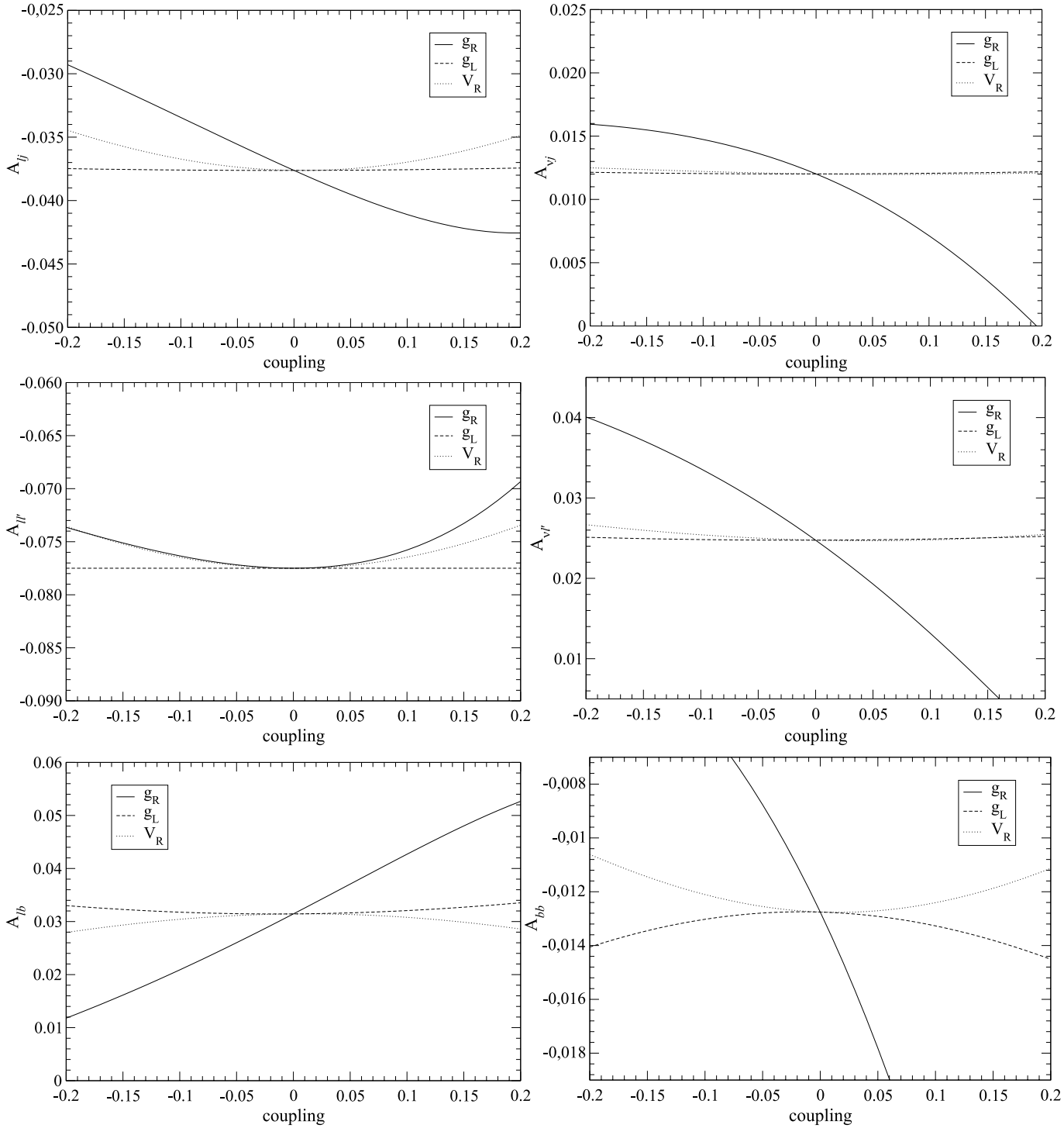

Fig. 6. Dependence of several spin correlation asymmetries on the couplings $g_{\rm R}$, $g_{\rm L}$ and $V_{\rm R}$, for the CP-conserving case

one loop $D = -0.238$ [29], with a theoretical uncertainty of $\sim 4\%$. Corresponding to these distributions, we can build the asymmetries

$$\tilde{A}_{X\bar{X}'} \equiv \frac{N(\cos\varphi_{X\bar{X}'} > 0) - N(\cos\varphi_{X\bar{X}'} < 0)}{N(\cos\varphi_{X\bar{X}'} > 0) + N(\cos\varphi_{X\bar{X}'} < 0)} = \frac{1}{2} D \alpha_X \alpha_{\bar{X}'} \,. \tag{23}$$

For charge conjugate decay channels the distributions can be summed, since $\alpha_{X'}\alpha_{\bar{X}} = \alpha_X \alpha_{\bar{X}'}$ provided CP is conserved in the decay. The dependence of these asymmetries $\tilde{A}_{X\bar{X}'}$ on anomalous couplings is (within the production $\times$ decay factorisation approximation) exactly the same as for the asymmetries $A_{X\bar{X}'}$ defined above, and plots are not presented for brevity. Simulations are available for $\tilde{A}_{\ell j}$ and $\tilde{A}_{\ell\ell'}$, whose theoretical SM values are $\tilde{A}_{\ell j} = 0.0527$,

$\tilde{A}_{\ell\ell'} = 0.1085$. The experimental precision expected [21, 24] is $\tilde{A}_{\ell j} \simeq 0.0554 \pm 0.0061$, $\tilde{A}_{\ell\ell'} \simeq 0.1088 \pm 0.0056$. This is a better precision than for $A_{\ell j}$ and $A_{\ell j}$, respectively, but still not competitive in the determination of the *Wtb* vertex structure.[5] Instead, we can use them to test top spin correlations. From these asymmetries one can extract the value of D, obtaining

$$\begin{aligned}\tilde{A}_{\ell\ell'} \to D = &-0.217 \pm 0.011\,(\mathrm{exp})\,{}^{+0.0031}_{-0.}\,(\delta V_\mathrm{R}) \\ &{}^{+2\times10^{-6}}_{-8\times10^{-6}}(\delta g_\mathrm{L})\,{}^{+0.0003}_{-0.}\,(\delta g_\mathrm{R})\,, \\ \tilde{A}_{\ell j} \to D = &-0.217 \pm 0.024\,(\mathrm{exp})\,{}^{+0.0047}_{-0.}\,(\delta V_\mathrm{R}) \\ &{}^{+0.0006}_{-9\times10^{-6}}(\delta g_\mathrm{L})\,{}^{+0.0004}_{-6\times10^{-5}}\,(\delta g_\mathrm{R})\,. \end{aligned} \tag{24}$$

The errors quoted correspond to the experimental (systematic + statistical) uncertainty and the variation when one of the anomalous couplings is allowed to be nonzero. As in the previous case, the measurement of a ratio of two asymmetries $\tilde{A}_{X\bar{X}'}$ provides a clean probe for anomalous couplings, but with a precision expected to be worse than for spin-independent observables.

6 Effect of complex phases in helicity fractions and spin asymmetries

In the previous sections we have assumed that any non-standard *Wtb* couplings are real, either positive or negative. We have also pointed out that, if a non-zero coupling g_R exists, its phase has an important influence on W helicity fractions and angular distributions determined by them. Complex phases in V_R, g_L and g_R influence the helicity fractions F_i through interference terms, which involve the real parts of these couplings (assuming V_L real). (Interference terms are the most important ones for small values of V_R, g_L and g_R, and for the latter coupling they are unsuppressed.) The maximum and minimum effects of anomalous couplings on F_i are obtained when they are real, negative or positive (not necessarily in this order). We show in Fig. 7 the values of the helicity fractions for fixed moduli and arbitrary phases of the new couplings, $V_\mathrm{R} = 0.1\,\mathrm{e}^{\mathrm{i}\phi_{V_\mathrm{R}}}$, $g_\mathrm{L} = 0.1\,\mathrm{e}^{\mathrm{i}\phi_{g_\mathrm{L}}}$, $g_\mathrm{R} = 0.1\,\mathrm{e}^{\mathrm{i}\phi_{g_\mathrm{R}}}$ (one different from zero at a time), to illustrate the effect of the phases. The plot scales have been enlarged to cover all the range of variation of F_i, and the 2σ expected limits have been marked with a gray dashed line.

For g_L and V_R the deviations from the SM value are relatively stable under variations of the phases, because the linear terms (which depend on the phase) and quadratic ones (which do not) are comparable in magnitude. Thus, the presence of a complex phase does not significantly affect the observability of the coupling. On the other hand, for g_R the effect of the phase is dominant, and we notice that for phases $\phi_{g_\mathrm{R}} = \pm\pi/2$ the helicity fractions are very close to their SM values, so that a purely imaginary coupling $g_\mathrm{R} \sim O(0.1)$ could remain unnoticed in an analysis of angular distributions. We also note that the plots are symmetric with respect to the y axis, because F_i depend on $\mathrm{Re}\,V_\mathrm{R}$, $\mathrm{Re}\,g_\mathrm{L}$, $\mathrm{Re}\,g_\mathrm{R}$ and the moduli. This also implies that complex couplings have the same effect on the helicity fractions in t and $\bar{t}$ decays. Therefore, the comparison in t and $\bar{t}$ decays of the angular distributions studied does not give any extra information regarding the complex phases, and further observables are needed in order to investigate this possibility. We have also analysed the phase dependence of the most interesting spin asymmetries, $A_{\ell j}$, $\tilde{A}_{\ell j}$, $A_{\ell\ell'}$ and $\tilde{A}_{\ell\ell'}$ (in semileptonic decays we consider $W^+ \to \ell^+\nu$, $W^- \to \bar{q}q'$). The effect of the phases is barely detectable, even with a greater experimental precision, and in any case the phase and modulus of an eventual anomalous coupling measured could not be disentangled.

[5] A special situation occurs if there is a fine-tuned cancellation between two nonzero V_R and g_L couplings leading to small effects in W helicity fractions and related quantities. These cancellations are possible, and in such particular case the measurement of spin asymmetries like $A_{\ell\ell'}$ and $\tilde{A}_{\ell\ell'}$ (which are insensitive to g_L but sensitive to V_R) or single top production may be used to obtain additional information about anomalous *Wtb* couplings.

7 CP-violating asymmetries

In this section we examine whether the existence of complex phases in the anomalous couplings can be detected using CP-violating asymmetries. The possibility of a relatively large imaginary coupling g_R is particularly intriguing, since angular distributions are very sensitive to this coupling provided its phase is not close to $\pm\pi/2$. For the other couplings, g_L and V_R, the situation is not so dramatic, because the observability mainly depends on their moduli.

The spin asymmetry [36]

$$A_\mathrm{CP}^\mathrm{RL} = \frac{\sigma(t_\mathrm{R}\bar{t}_\mathrm{R}) - \sigma(t_\mathrm{L}\bar{t}_\mathrm{L})}{\sigma(t_\mathrm{R}\bar{t}_\mathrm{R}) + \sigma(t_\mathrm{L}\bar{t}_\mathrm{L})}\,, \tag{25}$$

is CP-violating, and vanishes at the tree level in QCD interactions. The top and antitop spins can be inferred using their decay products as spin analysers, in the same way as in Sect. 5. We thus write

$$A_\mathrm{CP}^\mathrm{RL} = \frac{N(\cos\theta_X > 0, \cos\theta_{\bar{X}'} > 0) - N(\cos\theta_X < 0, \cos\theta_{\bar{X}'} < 0)}{N(\cos\theta_X > 0, \cos\theta_{\bar{X}'} > 0) + N(\cos\theta_X < 0, \cos\theta_{\bar{X}'} < 0)}\,. \tag{26}$$

Even with $A_\mathrm{CP}^\mathrm{LR}$ vanishing in the production process, complex phases in the decay could in principle lead to an observable asymmetry. We have considered the dilepton channel, in which larger asymmetries are expected because of the higher spin analysing power of the charged leptons. (Other possibility to measure this asymmetry in the dilepton channel would be to consider the charged lepton energies [37].) We have found that, for anomalous couplings of order $O(0.1)$ and arbitrary phases, this asymmetry remains below the permille level, and with values consistent

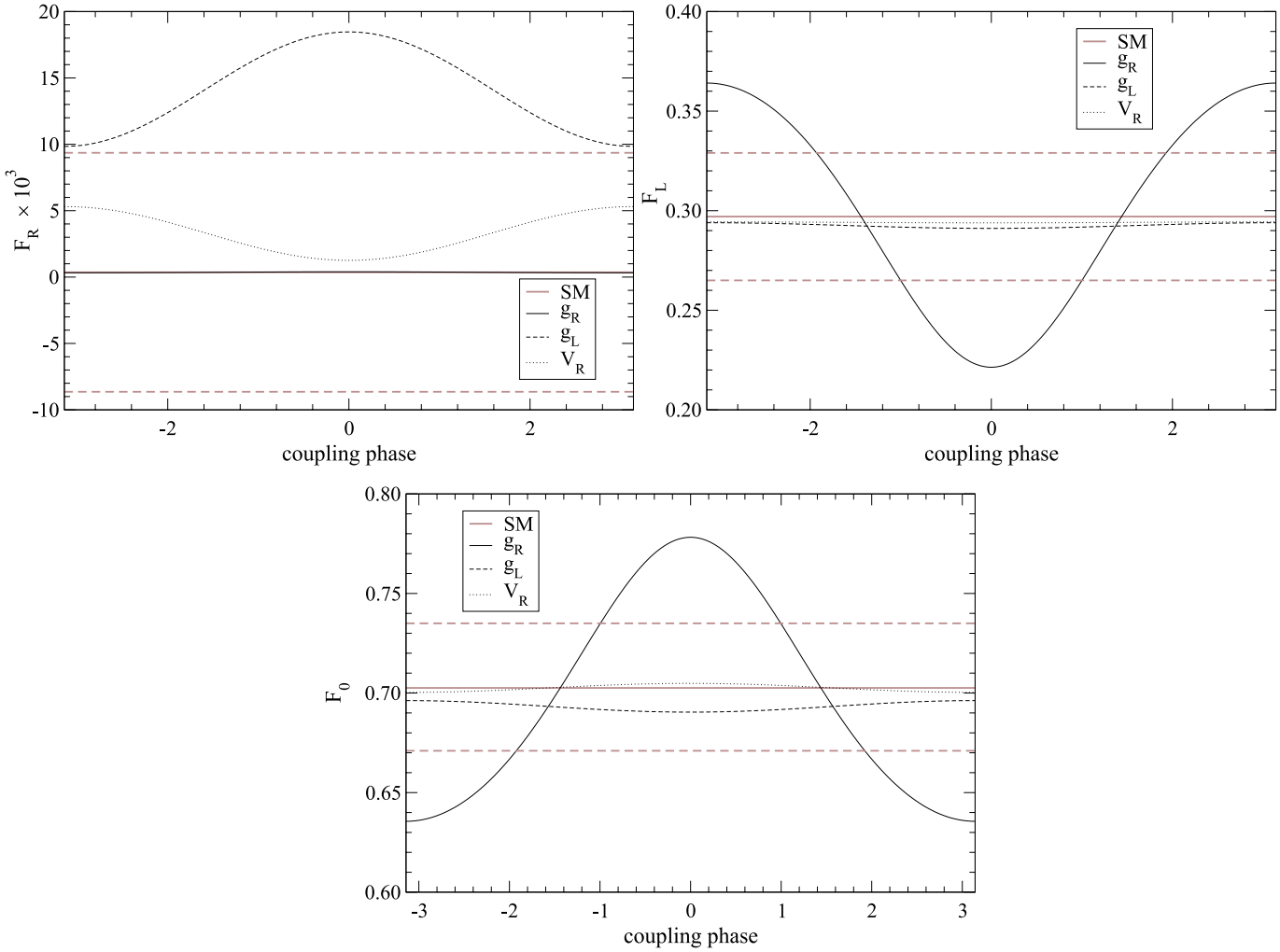

Fig. 7. Dependence of the helicity fractions F_i on the phases of the anomalous couplings (see the text for details)

with zero within Monte Carlo uncertainty. Observation of such asymmetry would then unambiguously indicate CP-violating effects in $t\bar{t}$ production, which are possible, for instance, in two Higgs doublet models [36, 38–40].

We also investigate triple-product asymmetries defined in the dilepton channel,

$$A_{\rm CP}^{T_i} = \frac{N(T_i > 0) - N(T_i < 0)}{N(T_i > 0) + N(T_i < 0)} \,, \tag{27}$$

where the triple products T_i are [38, 41]

$$\begin{aligned} T_1 &= \hat{\mathbf{e}} \cdot (\mathbf{p}_{\ell^+} - \mathbf{p}_{\ell^-}) \, (\mathbf{p}_{\ell^+} \times \mathbf{p}_{\ell^-}) \cdot \hat{\mathbf{e}} \,, \\ T_2 &= (\mathbf{p}_b - \mathbf{p}_{\bar{b}}) \cdot (\mathbf{p}_{\ell^+} \times \mathbf{p}_{\ell^-}) \,, \\ T_3 &= (\mathbf{p}_t - \mathbf{p}_{\bar{t}}) \cdot (\mathbf{p}_{\ell^+} \times \mathbf{p}_{\ell^-}) \,. \end{aligned} \tag{28}$$

The unit vector $\hat{\mathbf{e}}$ is taken in the beam direction and the particle momenta follow obvious notation. Final state particle momenta can be measured in the laboratory frame or, if the kinematics of the event is completely reconstructed, in other reference system. For asymmetries built using T_1 and T_3 we have found values $O(10^{-4})$, and compatible with zero, taking anomalous couplings of order $O(0.1)$ with arbitrary phases. On the other hand, we have found that $A_{\rm CP}^{T_2}$ is sensitive to a $g_{\rm R}$ coupling of this magnitude. The asymmetry is larger if the charged lepton and b quark momenta are measured in the respective rest frames of the decaying top quarks. However, its observability will depend on systematic errors associated to the reconstruction, which have not been estimated as yet, and may be better when defined in the laboratory frame. The asymmetry $A_{\rm CP}^{T_2}$ in both reference systems as plotted in Fig. 8, for couplings $g_{\rm R} = 0.05$, $g_{\rm R} = 0.1$ with arbitrary phases.

Other asymmetries discussed in the literature are based on the differences

$$\begin{aligned} \Delta_1 &= E_{\ell^+} - E_{\ell^-} \,, \\ \Delta_2 &= \mathbf{p}_{\bar{t}} \cdot \mathbf{p}_{\ell^+} - \mathbf{p}_t \cdot \mathbf{p}_{\ell^-} \,, \\ \Delta_3 &= \cos\theta_{\ell^+} - \cos\theta_{\ell^-} \,. \end{aligned} \tag{29}$$

These quantities do not involve the product $(\mathbf{p}_{\ell^+} \times \mathbf{p}_{\ell^-})$, and then they can be measured in the semileptonic channel too [41]. The asymmetries are built as in (27), and take values below the permille level for anomalous couplings of

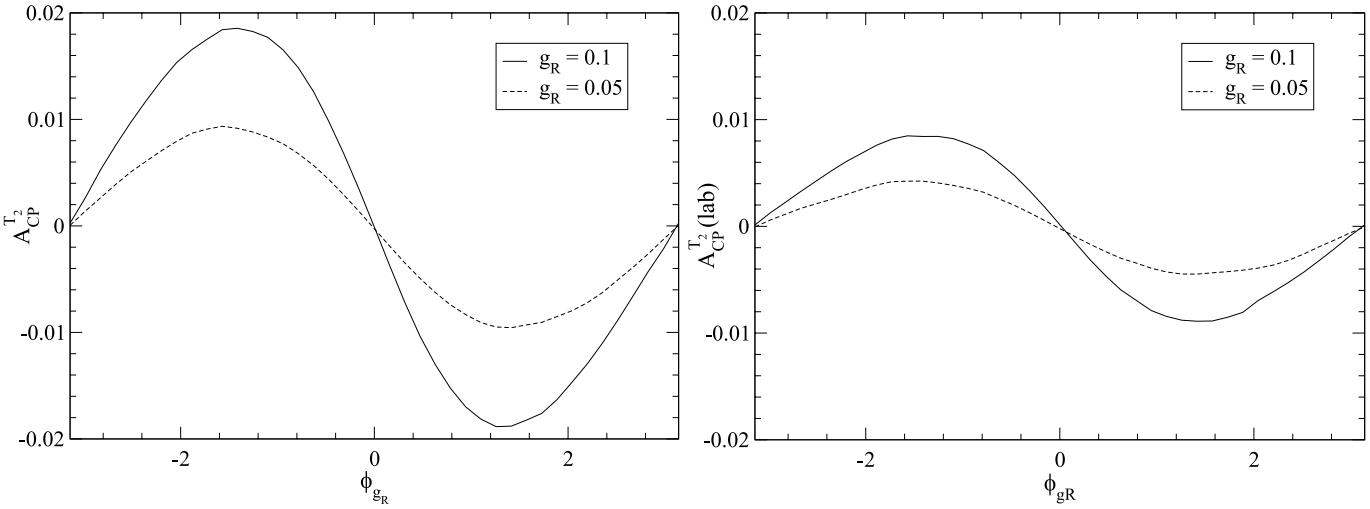

Fig. 8. Dependence of the CP asymmetry $A_{\rm CP}^{T_2}$, defined in top quark rest frame (*left*) and laboratory system (*right*), on the phase of $g_{\rm R}$

the size considered in this section. For completeness, we have also considered the P-violating asymmetry

$$A_{\rm P}^{\rm RL} = \frac{\sigma(t_{\rm R}\bar{t}_{\rm L}) - \sigma(t_{\rm L}\bar{t}_{\rm R})}{\sigma(t_{\rm R}\bar{t}_{\rm L}) + \sigma(t_{\rm L}\bar{t}_{\rm R})}\,, \tag{30}$$

which is measured using the charged leptons as spin analysers,

$$A_{\rm P}^{\rm RL} = \frac{N(\cos\theta_X > 0, \cos\theta_{\bar{X}'} < 0) - N(\cos\theta_X < 0, \cos\theta_{\bar{X}'} > 0)}{N(\cos\theta_X > 0, \cos\theta_{\bar{X}'} < 0) + N(\cos\theta_X < 0, \cos\theta_{\bar{X}'} > 0)}\,. \tag{31}$$

We have found $A_{\rm P}^{\rm RL} \sim 1.5 \times 10^{-3}$, and insensitive to anomalous couplings $O(0.1)$. This asymmetry can be sizeable in SM extensions [42].

We finally emphasise that, even in the cases where they are insensitive to complex anomalous *Wtb* couplings, the CP-violating asymmetries studied here are still very useful to disentangle CP violation in the production and the decay. If these asymmetries are found to be non-vanishing, they clearly signal CP violation in $t\bar{t}$ production. On the other hand, the imaginary part of $g_{\rm R}$ can be probed using $A_{\rm CP}^{T_2}$.

8 Summary

New physics, if it exists close to the electroweak scale, may manifest itself through non-standard top interactions. In this paper we have discussed top pair decays at LHC as a probe of the *Wtb* vertex. We have examined angular and energy distributions, as well as asymmetries, involving or not the top quark polarisation. Among the observables discussed, the best sensitivity to anomalous *Wtb* couplings is given by the W helicity fractions $F_i = \Gamma_i/\Gamma$, $i = {\rm L}, {\rm R}, 0$, and related observables. We have obtained analytical expressions for F_i, for a general CP-violating *Wtb* vertex with the top quark and W boson on their mass shell, and keeping a non-zero bottom quark mass. We have shown, comparing with exact numerical results, the high accuracy of this approximation when studying angular distributions. We have also pointed out the importance of keeping the bottom mass in the calculations, in contrast with previous studies in the literature.

W helicity fractions can be extracted from a fit to the charged lepton angular distribution in W rest frame. The same analysis can be used to determine the helicity ratios $\rho_{\rm R,L} = \Gamma_{\rm R,L}/\Gamma_0$, which are actually more sensitive to $V_{\rm R}$ and $g_{\rm L}$-type anomalous couplings, given the experimental uncertainties (dominated by systematics already for a luminosity of $10\,{\rm fb}^{-1}$) associated to each observable. A simpler method to probe the *Wtb* vertex, without the need of a fit to the charged lepton distribution, is through angular asymmetries. We have introduced two new asymmetries A_+ and A_-, in addition to the ℓW (or ℓb) forward–backward asymmetry $A_{\rm FB}$ previously studied [11]. These new asymmetries allow us to: (i) obtain more precise bounds on anomalous couplings than $A_{\rm FB}$, comparable with those obtained from $\rho_{\rm R,L}$ and F_i, and even better for a $g_{\rm R}$ coupling; (ii) determine the helicity fractions with a fair accuracy without fitting the charged lepton distribution. The W helicity fractions determine the charged lepton energy distribution in top rest frame as well. Energy asymmetries can be built, but they are less suited for the study of anomalous couplings because the approximation of considering the top quark and W boson on shell is worse, and experimental uncertainties on energy asymmetries are larger. The best limits found, using single measurements, are

$$\begin{aligned} &-0.029 \le V_{\rm R} \le 0.099 && (\rho_{\rm R})\,, \\ &-0.046 \le g_{\rm L} \le 0.013 && (\rho_{\rm R})\,, \\ &-0.019 \le g_{\rm R} \le 0.018 && (A_+)\,. \end{aligned} \tag{32}$$

Limits can be improved by combining the measurements of $A_\pm$ and $\rho_{\rm R,L}$. The theoretical predictions for these and

other observables have been implemented in a computer program TOPFIT, which allows to extract combined limits on anomalous couplings from a given set of observables, following the statistical approach outlined in Appendix B. Detailed results including the correlation of the various observables (computed from Monte Carlo simulations) are beyond the scope of this paper, and have been presented elsewhere [20].

Spin correlations and spin-dependent asymmetries probe not only the *Wtb* interactions but also the dynamics of $t\bar{t}$ production. Their study is very interesting from a theoretical point of view, because they are sensitive to e.g. the exchange of a scalar particle in s channel [43] or anomalous gtt couplings [44]. It is then crucial to disentangle new physics in the production from possible anomalous *Wtb* couplings. This could be done, for instance, considering ratios of spin correlation asymmetries or, even better, using the strict bounds on anomalous couplings obtained from top decay angular distributions.

The dependence of spin correlation asymmetries on *Wtb* anomalous couplings occurs through the "spin analysing power" constants of top quark decay products. We have calculated these constants for a general CP-conserving *Wtb* vertex, in the narrow width approximation. It has been shown that the sensitivity of spin correlation asymmetries to top anomalous couplings is much weaker than for helicity fractions and related observables. Then, we have set explicit limits on the variation of two factors C, D (which measure the $t\bar{t}$ spin correlation) due to possible anomalous couplings not detected in other processes, *i.e.* within the ranges in (32). The possible variation in C, D is much smaller than the experimental precision expected for their measurement,

$$\begin{aligned} C &= 0.310 \pm 0.024\,(\mathrm{exp})\,{}^{+0.}_{-0.0043}\,(\delta V_\mathrm{R}) \\ &\quad {}^{+1\times10^{-5}}_{-3\times10^{-6}}(\delta g_\mathrm{L})\,{}^{+7\times10^{-6}}_{-0.0004}\,(\delta g_\mathrm{R})\,, \\ D &= -0.217 \pm 0.011\,(\mathrm{exp})\,{}^{+0.0047}_{-0.}\,(\delta V_\mathrm{R}) \\ &\quad {}^{+0.0006}_{-9\times10^{-6}}(\delta g_\mathrm{L})\,{}^{+0.0004}_{-6\times10^{-5}}\,(\delta g_\mathrm{R})\,. \end{aligned} \tag{33}$$

Hence, any deviation observed experimentally should correspond to new physics in the production. On the other hand, in ratios of two spin asymmetries $A_{X\bar{X}'}$ ($\tilde{A}_{X\bar{X}'}$) the common factors C (D) cancel, and thus the ratios can cleanly probe non-standard top couplings. These observables have also been implemented in the computer program TOPFIT, and estimates for their expected precision will be presented elsewhere.

Finally, we have addressed the possibility of complex anomalous *Wtb* couplings g_L, g_R, V_R. Complex phases in these terms influence helicity fractions and related quantities via the interference with the dominant SM coupling V_L (which we have normalised to unity). For V_R and g_L, quadratic and interference terms have the same magnitude, and the effect of phases is not very relevant. For g_R, however, the interference term dominates, and the dependence on the phase is very strong. One finds that a g_R coupling with a phase close to $\pm\pi/2$ has little effect on angular distributions, and even with a relatively large modulus it could remain unnoticed in such analyses. The same has been found for spin correlation asymmetries. However, we have shown that a CP asymmetry based on the triple product $(\mathbf{p}_b - \mathbf{p}_{\bar{b}}) \cdot (\mathbf{p}_{\ell^+} \times \mathbf{p}_{\ell^-})$ is sensitive to a complex g_R, taking values up to $\pm 2\%$ for $g_\mathrm{R} = \mp 0.1\mathrm{i}$. If this asymmetry can be measured at LHC with a precision below the percent level, it could help to measure or bound g_R. The remaining CP asymmetries analysed are very small, and insensitive to anomalous couplings of this size. Therefore, they can be used to isolate CP violating effects in $t\bar{t}$ production [38–40]. On the other hand, single top production at LHC can probe the *Wtb* interaction, and B or super-B factories, with precise measurements of CP asymmetries e.g. in $b \to s\gamma$, might also give indirect evidence for (real or complex) anomalous *Wtb* couplings, helping to determine the structure of this vertex.

Acknowledgements. The work of J.A.A.-S. has been supported by a MEC Ramon y Cajal contract and project FPA2003–09298–C02–01, and by Junta de Andalucí a through project FQM-101. The work of J.C., N.C. (grant SFRH/BD/13936/2003), A.O. and F.V. (grant SFRH/BD/18762/2004) has been supported by Fundação para a Ciência e a Tecnologia.

Appendix A: Effect of m_b in the helicity fractions

As it can be observed in (2), interference terms involving V_R (or g_L) and the dominant SM coupling V_L are proportional to $x_b = m_b/m_t$. These terms are of equal size as the quadratic terms for small V_R, g_L, and cannot be neglected in the analysis. To illustrate their importance, we plot in Fig. 9 the dependence of the three helicity fractions on the anomalous couplings, for $m_b = 4.8$ GeV and neglecting m_b. The differences are apparent for F_R, and for F_0 we have the extreme situation that the only dependence of this quantity on V_R is through the x_b term.

The m_b dependence of the limits generates a small uncertainty due to the uncertainty in m_b, for which we use the b quark pole mass. This b mass definition has an ambiguity of the order of $\Lambda_\mathrm{QCD} \simeq 220$ MeV (for other definitions the uncertainty is smaller). The variation of the limits in (32) when m_b is taken as $4.8\,\mathrm{GeV} \pm \Lambda_\mathrm{QCD}$ is presented in Table 4 (we display additional digits in order to better illustrate the variation). The effect is larger for V_R and g_L, as it is expected from the discussion in Sect. 2. Nevertheless, the uncertainty only amounts to a few percent.

Appendix B: Extraction of limits from observables

The derivation of limits on the anomalous couplings from the measurement of the experimental observables discussed has to be done with special care, due to the non-linear dependence of the latter on the former. In this appendix we explain the method we have used to obtain our limits.

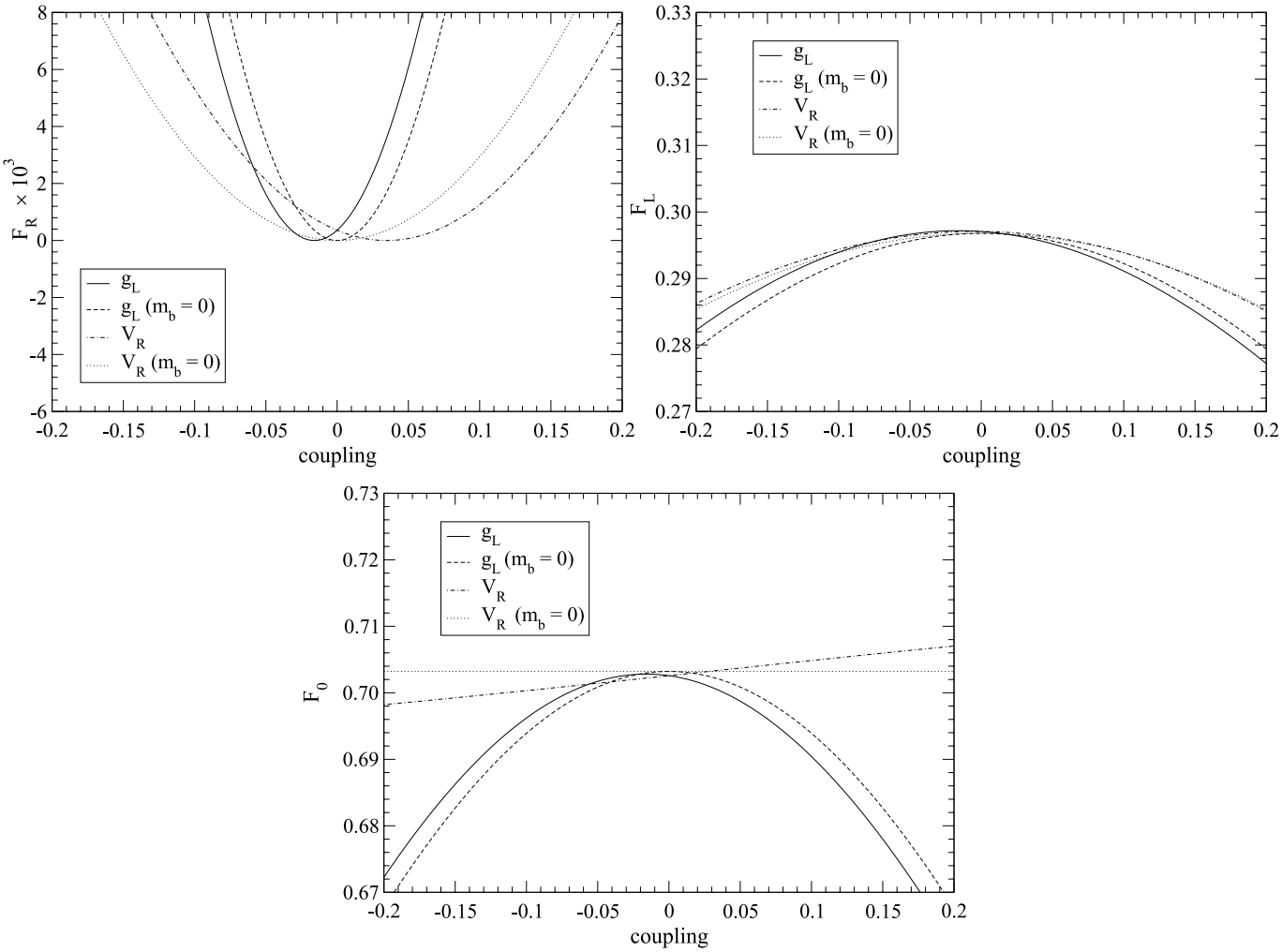

Fig. 9. Dependence of the helicity fractions F_i on $V_{\rm R}$ and $g_{\rm L}$, for $m_b = 4.8$ GeV and neglecting the b quark mass

Table 4. Influence of m_b in the limits in (32): variation when the b quark mass is taken at its central value $m_b = 4.8$ GeV, or adding and subtracting a small uncertainty $\Lambda_{\rm QCD} = 220$ MeV

	Lower limit			Upper limit		
Coupling	$m_b - \Lambda_{\rm QCD}$	m_b	$m_b + \Lambda_{\rm QCD}$	$m_b - \Lambda_{\rm QCD}$	m_b	$m_b + \Lambda_{\rm QCD}$
$V_{\rm R}$	−0.0303	−0.0293	−0.0281	0.0977	0.0994	0.1077
$g_{\rm L}$	−0.0444	−0.0456	−0.0461	0.0140	0.0135	0.0127
$g_{\rm R}$	−0.0192	−0.0194	−0.0192	0.0181	0.0180	0.0178

Let us denote by O a generic observable, e.g. an angular asymmetry, and x an unknown parameter (in our case an anomalous coupling) upon which this observable depends, and for which we want to obtain a confidence interval. O is experimentally measured and is assumed to obey a Gaussian distribution (with mean and standard deviation given by its measurement). However, if the dependence $O(x)$ is non-linear in the region of interest, the probability density function (p.d.f.) derived for the parameter x will no longer be a Gaussian and a Monte Carlo method must be used to determine a confidence interval on x.

We determine the p.d.f. of x numerically, using the acceptance-rejection method: we iteratively (i) generate a random value (with uniform probability) x_i within a suitable interval; (ii) evaluate the probability of $O(x_i)$, given by the p.d.f. of O; (iii) generate an independent random number r_i (with uniform probability); and (iv) accept the value x_i if the probability of $O(x_i)$ is larger than r_i. The resulting set of values $\{x_i\}$ is distributed according to the p.d.f. of x given by the measurement of O. The determination of a central interval with a given confidence level (CL) γ is done numerically, requiring: (a) that it contains a fraction γ of the total number of values $\{x_i\}$; (b) that is central, *i.e.* fractions $(1-\gamma)/2$ of the values generated are on each side of the interval.

We have applied this method to obtain the limits on Tables 1 and 2, keeping only one of the couplings non-vanishing at a time. We point out that:

1. The dependence on $g_{\rm R}$ of the observables F_i, $\rho_{\rm R,L}$, $A_\pm$ and $A_{\rm FB}$ is approximately linear, as it can be observed in Figs. 2–4. Therefore, the limits on this coupling can be approximately obtained directly from these plots using the method in [21, 24]: for a given observable O, intersecting the plot of $O(g_{\rm R})$ with the two horizontal lines $O = O_{\rm exp} \pm \Delta O$, which correspond to the 1σ variation of O, gives the 1σ interval (with a 68.3% CL) on $g_{\rm R}$.
2. The dependence on $g_{\rm L}$ and $V_{\rm L}$ is highly non-linear (the region of interest is at the extreme of a quadratic function), and appreciable differences are found between the Monte Carlo and the intersection methods. For example, the "1σ" limit on $V_{\rm R}$ obtained with the intersection method from the (hypothetical) measurement $\rho_{\rm R} \simeq 0.0005 \pm 0.0026$ is $-0.051 \leq V_{\rm R} \leq 0.12$. However, this interval has a confidence level of 85.6%, and the true 68.3% central interval obtained from the same measurement with the Monte Carlo method outlined above is $-0.029 \leq V_{\rm R} \leq 0.099$. Although overcoverage is not as bad as undercoverage, it is quite desirable that confidence intervals have exactly the CL they are supposed to have.

A similar procedure is applied to estimate the theoretical uncertainties in (21) and (24) due to possible anomalous couplings.

References

1. M. Beneke et al., hep-ph/0003033
2. T. Stelzer, Z. Sullivan, S. Willenbrock, Phys. Rev. D **58**, 094021 (1998) [hep-ph/9807340]
3. A.S. Belyaev, E.E. Boos, L.V. Dudko, Phys. Rev. D **59**, 075001 (1999) [hep-ph/9806332]
4. T. Tait, C.P. Yuan, Phys. Rev. D **63**, 014018 (2001) [hep-ph/0007298]
5. E. Boos, M. Dubinin, A. Pukhov, M. Sachwitz, H.J. Schreiber, Eur. Phys. J. C **21**, 81 (2001) [hep-ph/0104279]
6. J.A. Aguilar-Saavedra, Phys. Rev. D **67**, 035003 (2003)
7. J.A. Aguilar-Saavedra, Phys. Rev. D **69**, 099901 (2004) [Erratum, hep-ph/0210112]
8. F. del Aguila, J. Santiago, JHEP **0203**, 010 (2002) [hep-ph/0111047]
9. J.J. Cao, R.J. Oakes, F. Wang, J.M. Yang, Phys. Rev. D **68**, 054019 (2003) [hep-ph/0306278]
10. X.L. Wang, Q.L. Zhang, Q.P. Qiao, Phys. Rev. D **71**, 014035 (2005) [hep-ph/0501145]
11. F. del Aguila, J.A. Aguilar-Saavedra, Phys. Rev. D **67**, 014009 (2003) [hep-ph/0208171]
12. H.S. Do, S. Groote, J.G. Korner, M.C. Mauser, Phys. Rev. D **67**, 091501 (2003) [hep-ph/0209185]
13. Particle Data Group, S. Eidelman et al., Phys. Lett. B **592**, 1 (2004)
14. F. Larios, M.A. Perez, C.P. Yuan, Phys. Lett. B **457**, 334 (1999) [hep-ph/9903394]
15. G. Burdman, M.C. Gonzalez-Garcia, S.F. Novaes, Phys. Rev. D **61**, 114016 (2000) [hep-ph/9906329]
16. K. Whisnant, J.M. Yang, B.L. Young, X. Zhang, Phys. Rev. D **56**, 467 (1997) [hep-ph/9702305]
17. M. Misiak, private communication, to appear in the proceedings of the workshop "Flavour in the era of the LHC", CERN 2005–2007
18. D. Espriu, J. Manzano, Phys. Rev. D **66**, 114009 (2002) [hep-ph/0209030]
19. C.R. Chen, F. Larios, C.P. Yuan, Phys. Lett. B **631**, 126 (2005) [AIP Conf. Proc. **792**, 591 (2005), hep-ph/0503040]
20. J.A. Aguilar-Saavedra, J. Carvalho, N. Castro, A. Onofre, F. Veloso, ATLAS note ATL-PHYS-PUB-2006-031, http://cdsweb.cern.ch/record/975938
21. J.A. Aguilar-Saavedra, J. Carvalho, N. Castro, A. Onofre, F. Veloso, ATLAS note ATL-PHYS-PUB-2006-018, http://cdsweb.cern.ch/record/952732
22. G.L. Kane, G.A. Ladinsky, C.P. Yuan, Phys. Rev. D **45**, 124 (1992)
23. R.H. Dalitz, G.R. Goldstein, Phys. Rev. D **45**, 1531 (1992)
24. F. Hubaut, E. Monnier, P. Pralavorio, K. Smolek, V. Simak, Eur. Phys. J. C **44S2**, 13 (2005) [hep-ex/0508061]
25. B. Lampe, Nucl. Phys. B **454**, 506 (1995)
26. M. Jezabek, Nucl. Phys. B Proc. Suppl. **37**, 197 (1994) [hep-ph/9406411]
27. A. Czarnecki, M. Jezabek, J.H. Kuhn, Nucl. Phys. B **351**, 70 (1991)
28. A. Brandenburg, Z.G. Si, P. Uwer, Phys. Lett. B **539**, 235 (2002) [hep-ph/0205023]
29. W. Bernreuther, A. Brandenburg, Z.G. Si, P. Uwer, Nucl. Phys. B **690**, 81 (2004) [hep-ph/0403035].
30. B. Grzadkowski, Z. Hioki, Phys. Lett. B **476**, 87 (2000) [hep-ph/9911505]
31. B. Grzadkowski, Z. Hioki, Phys. Lett. B **557**, 55 (2003) [hep-ph/0208079]
32. T. Stelzer, S. Willenbrock, Phys. Lett. B **374**, 169 (1996) [hep-ph/9512292]
33. G. Mahlon, S.J. Parke, Phys. Rev. D **53**, 4886 (1996) [hep-ph/9512264]
34. CTEQ Collaboration, H.L. Lai et al., Eur. Phys. J. C **12**, 375 (2000) [hep-ph/9903282]
35. M. Jezabek, J.H. Kuhn, Phys. Lett. B **329**, 317 (1994) [hep-ph/9403366]
36. C.R. Schmidt, M.E. Peskin, Phys. Rev. Lett. **69**, 410 (1992)
37. B. Grzadkowski, Z. Hioki, Nucl. Phys. B **484**, 17 (1997) [hep-ph/9604301]
38. W. Bernreuther, A. Brandenburg, Phys. Lett. B **314**, 104 (1993)
39. W. Khater, P. Osland, Nucl. Phys. B **661**, 209 (2003) [hep-ph/0302004]
40. A.W.E. Kaffas, W. Khater, O.M. Ogreid, P. Osland, hep-ph/0605142
41. W. Bernreuther, A. Brandenburg, Phys. Rev. D **49**, 4481 (1994) [hep-ph/9312210]
42. C. Kao, D. Wackeroth, Phys. Rev. D **61**, 055009 (2000) [hep-ph/9902202]
43. W. Bernreuther, M. Flesch, P. Haberl, Phys. Rev. D **58**, 114031 (1998) [hep-ph/9709284]
44. K.M. Cheung, Phys. Rev. D **55**, 4430 (1997) [hep-ph/9610368]